Uluslararası İleri Doğa Bilimleri ve Mühendislik Araştırmaları Dergisi
Sayı 9, S. 122-131, 10, 2025

Araştırma Makalesi

IJANSER

https://as-proceeding.com/index.php/ijanser
ISSN:2980-0811

International Journal of Advanced Natural Sciences and Engineering Researches
Volume 9, pp. 122-131, 10, 2025

Research Article

Heat Transfer Analysis of Radiative MHD Casson Fluid over Nonlinear Extended Sheet under Influence of Suction/Injection: non Similarity Numerical Investigation

Saqib Hussain[1], and Sidra Rana[*1]

[1]*Department of Mathematics, Faculty of Basic Sciences, University of Wah, Wah Cantt, Pakistan*

[*]*(sidra.rana@uow.edu.pk)*

(Received: 30 September 2025, Accepted: 05 October 2025)

(5th International Conference on Frontiers in Academic Research ICFAR 2025, September 25-26, 2025)

ATIF/REFERENCE: Hussain, S. & Rana, S. (2025). Heat Transfer Analysis of Radiative MHD Casson Fluid over Nonlinear Extended Sheet under Influence of Suction/Injection: non Similarity Numerical Investigation, *International Journal of Advanced Natural Sciences and Engineering Researches*, 9(10), 122-131.

Abstract – The present study investigates the heat transfer characteristics of radiative magnetohydrodynamic (MHD) Casson fluid flow over a nonlinear extended sheet subject to suction and injection effects. A non-similarity approach is employed to capture the more general behavior of the governing boundary layer equations, which are derived under appropriate physical assumptions. The mathematical model incorporates the influence of magnetic field, thermal radiation, nonlinear stretching, and suction/injection on the velocity and thermal boundary layers. By applying suitable similarity and non-similarity transformations, the governing partial differential equations are reduced to a coupled system of nonlinear equations, which are then solved numerically. The effects of key controlling parameters including the Casson parameter, magnetic field strength, nonlinear stretching index, radiation parameter, and suction/injection parameter on the flow and thermal distributions are analyzed in detail. The results highlight that suction enhances the cooling rate by thinning both velocity and thermal boundary layers, while injection produces the opposite effect. Moreover, the interaction between radiation and MHD significantly alters the heat transfer rate near the sheet. The findings provide useful insights into the control of transport phenomena in industrial processes involving polymer extrusion, coating, and cooling technologies.

Keywords – Casson Fluid, Nonlinear Stretching Sheet, Thermal Radiation, Suction And Injection, Non-Similarity Transformation.

I. INTRODUCTION

The applications of MHD flow are in nuclear reactors, petroleum industry, MHD generators, power production, and polymer production, which makes MHD flow a widely studied subject. The effect of MHD on the problem of stretching sheet was originally investigated by [1] and the subsequent studies took into account viscoelastic fluids with the presence of radiation[2]. In analyzed inclined MHD flow with radiation and CNT effects, where porous media Casson MHD flow has been studied [3-5]. Hybrid nanofluids and bio-convective flows were studied by Shamshuddin et al. [6]], which indicated that it was useful in industry under MHD fields. Among numerous non-Newtonian fluids, Casson fluid is a elastic solid at small shear stress and is able to flow only when the stress exerted is more than a specific yield value. Casson model was initially used to predict the flow of pigment-oil suspension and can also be applied to other fluids such as honey, soup, tomato sauce, concentrated juices, jelly and even human blood. Among others, C-O Ng et al. [7] was recently able to examine electroosmotic flow of Casson fluid in a slit microchannel, and B. Jalili [8] was able to study the nonlinear radiation effects in Casson squeezing flow in parallel disks. Hussain et al. reported the boundary layer flow of MHD, slip, and radiation of Casson fluid over stretching or shrinking surfaces[9].Boundary layer flow The flow of fluid with stretching or shrinking surfaces is significant in such processes as polymer extrusion, plastic film drawing, crystal growing or paper production. Other researchers like Khan et al. [10, 11] studied unsteady flows over expanding or contracting surfaces with nonlinear stretching, stagnation point flows and second-grade fluids. Boundary layer heat transfer is greatly altered by thermal radiation. Mahabaleshwar et al. [12] experimented flow and heat transfer of MHD including radiative effects. Additional developments of the Mahabaleshwar et al. [13] models were CNT-based models of mass transpiration and radiation. Sumithra [14] and Yesodha and Isah [15-17] studied the role of radiation in combination with chemical reactions and activation energy as important mechanisms of bounding the thickness of the boundary layer. It has been found that suction and injection impact on stability and heat transfer respectively. Vanitha et al. [18] researched on mass transpiration (suction/injection) using radiation in CNT-based MHD flows. The other works by the authors, including Khan et al. [19] and Akshatha et al. [20], investigated the suction/injection stretching sheet flows with nanoparticles.

Stretching sheet flows are a topic of central heat transfer problems because it has industrial applications in polymer processing, cooling systems and coating technologies. The research by Saleem et al. [21], Ashraf et al. [22], and Reddy et al. [23] took into account unsteady heat transfer in MHD Casson fluids and stagnation-point flows. Sudarsana Reddy et al. [24] studied combined heat and mass transfer with chemical reaction and Goud et al. [25] added to the activation energy influences in convective heat transfer. Stretching sheet problems have also been mentioned where entropy generation and radiative heat transfer have been noted [26-30].

The simplification of the boundary layer PDEs to ODEs by similarity transformations is frequently applied to simplify the equations, whereas non-similarity methods offer more generic results. The first liquid film flows to undergo similarity techniques were used by Wang [32], and later applied to nonlinear fluids and radiative effects by Wang [33-39]. As recently, Awad et al. [35] used spectral relaxation techniques of unsteady flows with binary chemical reaction and activation energy. Nanofluid models, Casson flows and the stretching sheet problems that involve complicated physical effects have also been addressed using non-similarity methods.

The primary purpose of this study is to conduct non-similarity numerical study of the heat transfer properties in radiative magnetohydrodynamic (MHD) Casson fluid flow around a nonlinear extended sheet under the forces of suction and injection. The present study is guided by the investigation of MHD forces, radiation, and fluid rheology in combination with wall mass transfer conditions to study the velocity and temperature distributions. The study also aims at offering correct numerical information on the boundary layer behavior which may be used as a guide towards real-worlds application in thermal engineering and other advanced material processing designs.

II. MATERIALS AND METHOD

Let us examine the heat transfer from a stretching sheet to an electroconductive polymer at the stagnation point y = 0 via MHD viscous, incompressible, steady-state boundary layer flow, and thermal convection. It makes use of the Casson fluid model. Because of the low magnetic Reynolds number, the induced magnetic field is disregarded and an external magnetic field B0 is supplied. There is very little electron pressure. The magnetic field is strong enough to create a Hall current, which causes ion-slip and a secondary flow (cross flow). As illustrated in Figure 1, a Cartesian coordinate system is used, where the x-axis is taken along the sheet's direction and the y-axis is regarded as normal to it. The temperature in the free stream is $\tilde{}$ ∞ T, whereas the temperature at the sheet is indicated by $\tilde{}$ Tw. A radiative flux is delivered transversely to the sheet, and it is assumed that the polymer is optically dense.

The regime's governing boundary layer equations can be expressed as follows

$$\frac{\partial u}{\partial x}+\frac{\partial v}{\partial y}=0, \quad (1)$$

$$u\frac{\partial u}{\partial x}+v\frac{\partial u}{\partial y}=\nu\left(1+\frac{1}{\beta}\right)\frac{\partial^2 u}{\partial y^2}+\frac{\sigma B_0^2}{\rho_{nf}}(u-U(x)), \quad (2)$$

$$u\frac{\partial T}{\partial x}+v\frac{\partial T}{\partial y}=\left[\alpha\left(\frac{\partial^2 T}{\partial y^2}\right)-\frac{1}{\rho c_p}\frac{\partial q_r}{\partial y}\right] \quad (3)$$

The appropriate conditions of boundary are as follow,

$$\left.\begin{array}{l} \mathrm{u}=\pm c x^m, \mathrm{v}=\mathrm{v_w}, \quad T=T_\infty+b x^{2m}, \quad \text{at } \ \mathrm{y}=0, \\ \mathrm{u}\rightarrow \mathrm{a x^m}, \quad \mathrm{v}\rightarrow 0\ , \quad \mathrm{T}\rightarrow T_\infty\,, \ \text{at} \ \ \mathrm{y}\rightarrow\infty\,. \end{array}\right\} \quad (4)$$

Using the Rosseland diffusion approximation, the nonlinear radiative heat flux can be expressed as follows:

$$q_r=-\frac{16\sigma T^3}{3k}\frac{\partial T}{\partial y}. \quad (5)$$

The stream function (ψ) can be defined as:

$$u=\frac{\partial\psi}{\partial y}, v=-\frac{\partial\psi}{\partial x} \quad (6)$$

The appropriate similarity variables is,

$$\xi=\frac{\sigma B_0^2 x}{\rho u_w(x)}, \psi=\sqrt{\frac{2\nu x u_w(x)}{(m+1)}}f(\xi,\eta), \eta=\sqrt{\frac{(m+1)u_w(x)}{2\nu x}}y, \\ \theta(\xi,\eta)=\frac{T-T_\infty}{T_w-T_\infty}, \quad (7)$$

where the stream function ψ and ν is the kinematic viscosity, which identically satisfies the Eq. (1). Substituting Eqs. (5)–(7) into Eqs. (2)–(4), we get following nonlinear ODEs:

$$\left(1+\frac{1}{\beta}\right)\frac{m+1}{2}f'''+\frac{m+1}{2}ff''-m(f'^2)-\xi\left(f'-\frac{\alpha}{c}\right)=(1-m)\xi\left(f'\frac{\partial f'}{\partial\xi}-f''\frac{\partial f}{\partial\xi}\right), \quad (8)$$

$$\frac{m+1}{2Pr}(1+Rd)\theta''+\frac{m+1}{2}f\theta'-2mf'\theta=(1-m)\xi\left(F'\frac{\partial\theta}{\partial\xi}-\theta'\frac{\partial F}{\partial\xi}\right), \quad (9)$$

Their corresponding BCs are:

$$\left\{\begin{array}{ll} f(0)=S,\ f'(0)=\pm1, \quad \theta(0)=1, & at\ \eta=0, \\ \qquad f'(\infty)\rightarrow\frac{a}{c},\quad \theta(\infty)\rightarrow 0\,, & as\ \ \eta\rightarrow\infty. \end{array}\right\}, \quad (10)$$

Here $Rd=\frac{16\sigma^* T_\infty{}^3}{3kk^*}$ is symbolized as radiation parameter, $\xi=\frac{\sigma B_0{}^2}{a\rho}$ is magnetic parameter, $\Pr=\frac{\nu}{\alpha}$ is Prandtl number, $S=\frac{2u_w(x)\cdot x^{-(m-1)/2}}{(m+1)\sqrt{c\nu}}$ suction/injection number.

The local Nusselt number and the skin friction coefficient are the physical quantities of importance for the governing flow problem. These values have the following dimensionless definitions:

$$C_F=C_f Re_x^{1/2}=\left(1+\frac{1}{\beta}\right)\left(\frac{m+1}{2}\right)f''(\xi,0), Nu_r=\frac{Nu}{Re_x^{1/2}}=-\left(\frac{m+1}{2}\right)^{\frac{1}{2}}\left(1+\frac{4}{3}Rd\right)\theta'(\xi,0), \quad (11)$$

whereas $Re_x=u_w x/\nu$ is the local Reynolds parameter.

A. *Local non-similarity technique*

The technique of local non-similarity used to solving Eqs. (4.09) through (4.10) is the next topic we cover. This equation's second-level truncation yields results that are almost as accurate as those obtained using the other techniques. We introduce the following new functions in order to accomplish this:

$$N=\frac{\partial F}{\partial\xi}, Z=\frac{\partial\theta}{\partial\xi}, \quad (12)$$

By adding the functions (4.13) to Eqs. (4.09) through (4.10), we obtain

$$\left(1+\frac{1}{\beta}\right)\frac{m+1}{2}f'''+\frac{m+1}{2}ff''-m(f'^2)-\xi\left(f'-\frac{\alpha}{c}\right)=(1-m)\xi(f'N'-f''N), \quad (13)$$

$$\frac{m+1}{2Pr}(1+Rd)\theta''+\frac{m+1}{2}f\theta'-2mf'\theta=(1-m)\xi(f'Z-\theta'\mathrm{N}), \quad (14)$$

Eliminating the terms containing the derivative functions N and Z with respect to ξ and differentiating Eqs. (13)–(14) with respect to ξ, we arrive at:

$\left(1+\frac{1}{\beta}\right)\frac{m+1}{2}N''' + \frac{m+1}{2}(fN''+Nf'') - 2mf'N' - \left(f' - \frac{\alpha}{c}\right) = (1-m)[(f'N' - f''N) + \xi(N'^2 - N''N)],$ (15)

$\frac{m+1}{2Pr}(1+Rd)Z'' + \frac{m+1}{2}(fZ'+N\theta') - 2m(f'Z+N'\theta) = (1-m)[\xi(N'Z - Z'\mathrm{N}) + (f'Z - \theta'\mathrm{N})],$ (16)

Differentiating the BCs (5.11) with respect to ξ ,we get

$N(\xi,\eta) = 0, N'(\xi,\eta) = 0, Z(\xi,\eta) = 0,$

$N'(\xi,\eta) \to 0, Z(\xi,\eta) \to 0.$

B. *Figures and Tables*

.

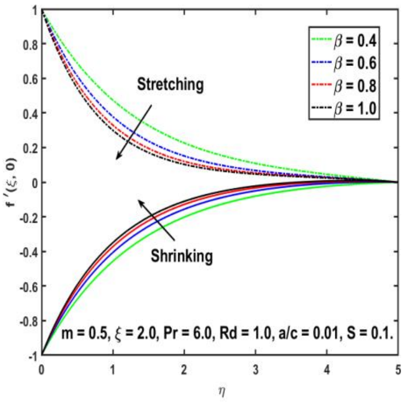

Fig. 2 Impact of β on $f'(\xi,0)$

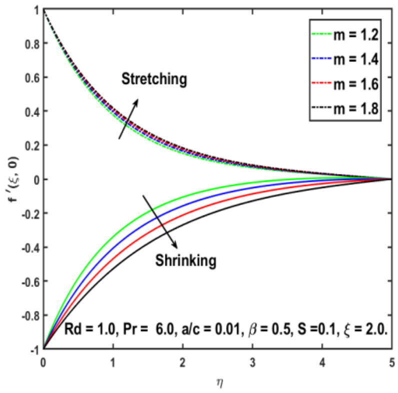

Fig. 3 Impact of m on $f'(\xi,0)$

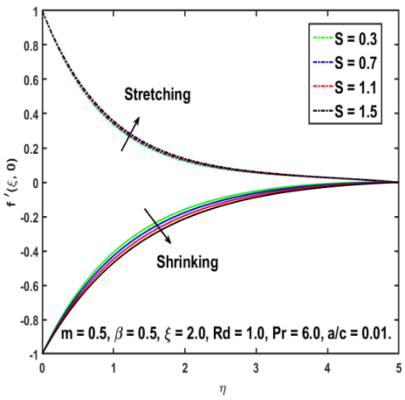

Fig. 4 Impact of S on $f'(\xi,0)$

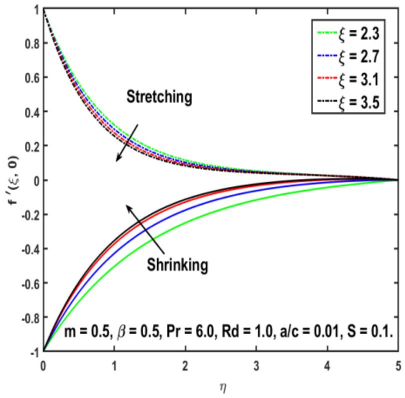

Fig. 5 Impact of ξ on $f'(\xi, 0)$

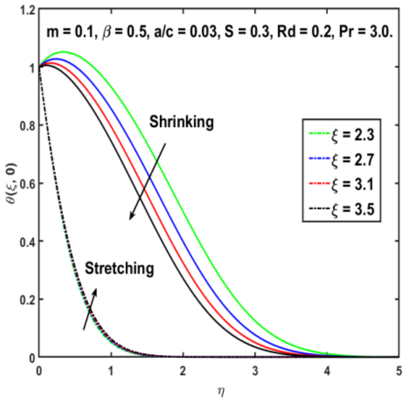

Fig. 6 Impact of ξ on $\theta(\xi, 0)$

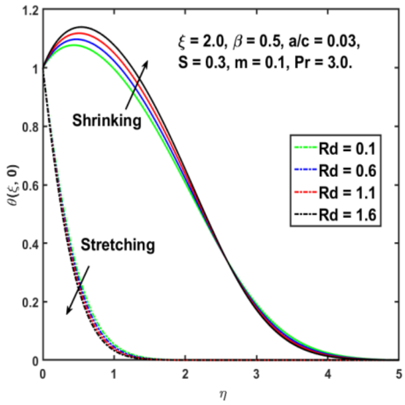

Fig. 7 Impact of Rd on $\theta(\xi, 0)$

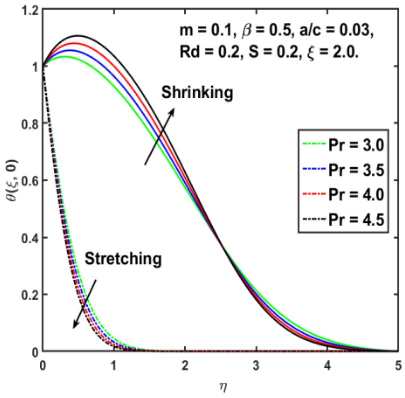

Fig. 8 Impact of Pr on $\theta(\xi, 0)$

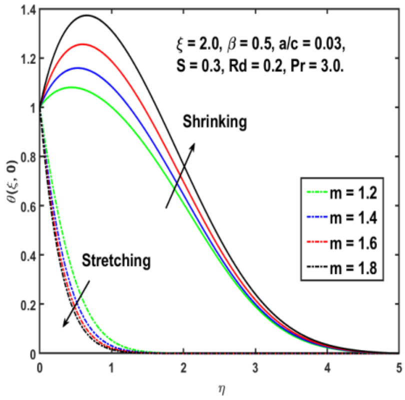

Fig. 9 Impact of m on $\theta(\xi, 0)$

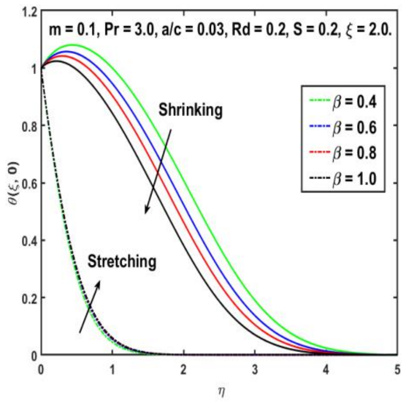

Fig. 10 Impact of β on $\theta(\xi, 0)$

Table 1. Numerical data for Nusselt number

Rd	Pr	m	β	ξ	Nu_x
0.3	1.0	1.0	0.8	0.3	1.588891
0.5					1.986783
0.7					2.411307
0.2	1.2				1.474096
	1.3				1.509955
	1.4				1.545185
	0.1	1.2			1.644598
		1.4			1.898132
		1.6			2.160895
		1.0	1.0		1.40171
			1.3		1.403246
			1.6		1.404358
			0.8	0.6	1.34959
				0.7	1.339677
				0.8	1.330396

Table 2: Numerical data for Skin friction number.

S	β	M	ξ	C_f
1.5	0.8	1.0	0.3	1.242871
2.5				1.236554
3.0				1.231468
1.0	1.3			1.23379
	1.8			1.224018
	2.3			1.217773
	0.8	1.4		1.264249
		1.6		1.269414
		1.8		1.273821
		1.0	0.5	1.366989
			0.7	1.473813
			0.9	1.573163

III. RESULTS & DISCUSSION

Figure 2 shows how different β influences the velocity field $f'(\xi,0)$ in the case of a shrinking and a stretching surface. The Casson parameter β is a dimensionless parameter that characterises non-Newtonian behaviour of Casson fluids, which are shear-thinning fluids and have yield stress, i.e. they act as a solid at low shear stress, and a fluid at high shear stress. It is noted that the greater the β, the lesser the velocity in the stretching case and the greater the velocity in the shrinking case. Physically the effect of increasing 2 is that it alters the effect of yield stress and the fluid tends to act more like a Newtonian fluid resulting in the slower velocity of stretching flows and the faster velocity of shrinking flows. As illustrated in Figure 3, the effect of m on the velocity field $f'(\xi, 0)$ is as follows: A dimensionless value, m is the power-law parameter describing the change in velocity of the stretching or shrinking surface. It is noted that an increase in the value of m increases the velocity in the stretching case, and decreases the velocity in the shrinking case. At the physical level, an increase in m increases the rate of stretching of the surface, which enhances the momentum boundary layer and accelerates the fluid at the stretching regime. On the other hand, the shrinking region, the greater the m the greater the inward pulling effect that smothers the flow and decreases the velocity. The effect of S on the velocity field $f'(\xi, 0)$ of Fig. 4 is exhibited. S Suction/injection parameter S is a dimensionless measure that illustrates the velocity of fluid suction (S>0) or injection (S<0) at the surface that has a direct impact on the thickness of the boundary layer and flow behavior. It is noted that the further the S the higher the velocity in the stretching case and the lower the velocity in the shrinking case. The effect of greater suction (S>0) is physical, and it eliminates the particles of the fluid in the boundary layer, thus stabilizes the flow and increases velocity on a stretching surface. In shrinking case, on the other hand, the fluid motion along the wall is suppressed by stronger suction, which decreases the velocity.

The effects of ξ on the velocity field $f'(\xi,0)$ are given in figure 5. Magnetic parameter ξ is a non-dimensional number that will quantify the effect of a transverse magnetic field on the flow of an electrical carrying fluid, commonly defined as the magnetic interaction effect. It is noted that the higher the value of ξ, the lower was the velocity in the stretching case and the higher was the velocity in the shrinking case. Physically, the magnetic field implemented creates a force known as Lorentz force which opposes the movement of the fluid, which decelerates the velocity in extending flows. But, in small currents, the effect of resistance is the opposite, and the great inward movement is opposed, as a consequence, thus stabilizing the current, and increasing the velocity of it. Therefore, magnetic parameter ξ is important in controlling the momentum boundary layer in the MHD fluid flows.

Figure 6 shows the influence of ξ of the temperature distribution of 6. It is noted that when ξ increases, the temperature increases in the stretching case but on the contrary, the temperature drops in the shrinking case. In the stretching flows the magnetic field applied induces a Lorentz force that opposes movements in the fluids causing more viscous dissipation and heat generation, heating the fluid. Conversely, in receding flows, the magnetic field overpowers the inducting motion, lowers the accumulation of thermal energy and causes lower temperature. Therefore, the magnetic parameter ξ plays an important role in determining the thermal boundary layer properties in MHD flows.

The radiation parameter Rd is a non-dimensional parameter that measures the contribution to heat transfer in the fluid flow of the thermal radiation, defined usually by the Rosseland approximation to the radiative heat flux. Figure 7 demonstrates how Rd affects the temperature profile $\theta(\xi,0)$. It is found that the higher the Rd, the lower is the temperature in the stretching case and the higher the temperature in the shrinking case. In the case of radiating flows, physically, when the Rd increases in stretching flows, radiative heat loss to the fluid increases, decreasing the thermal energy and lowering the temperature. In the shrinking flows on the other hand, the fluid layers are forced together and the action of radiative energy adds to the accumulation of thermal energy which in turn increases the temperature. Therefore, radiation parameter Rd is a crucial one to adjust the thermal boundary layer behavior in the case of stretching or shrinking surface conditions.

The Prandtl number Pr is a non-dimensional ratio of the viscosity of a medium (diffusion of momentum, or kinematic viscosity) to the thermal viscosity and is defined as Pr= ν / 20, and is used to describe the relative thickness of the velocity and thermal boundary layers. Figure 8 shows the impact of Pr on temperature distribution $\theta(\xi,0)$. It is seen that with increase of Pr, the temperature in the stretching case lowers whereas in the shrinking case it rises. Physically, in the stretching flows, increasing Pr leads to the decrease of thermal diffusivity, which thins thermal boundary layer and decreases the temperature. However, in shrinking flows the lower diffusivity of thermal energy due to decreasing flow combined with the inward motion causes one to get more heat at the surface, and the temperature of the fluid increases. Therefore, Prandtl number Pr is an important parameter in the regulation of heat transfer features in boundary layer flows.

The effect of m on the temperature field $\theta(\xi,0)$ is given in figure 9. It is noticed that the temperature is lowering in case of stretching whereas in the case of shrinking it is rising as m is increasing. Physically in the case of stretching flows, increasing m increases the rate of stretching which increases velocity of the fluid, decreases the thickness of the thermal boundary layer and lowers temperature. Conversely, when flows are shrinking, then a stronger m also enhances the inward movement, compresses the layers of fluid and holds more heat near the wall which heats the fluid. The power-law parameter mmm therefore plays a major role in determining the thermal boundary layer behaviour in both the shrinking and stretching regimes.

The impact of β in the temperature profile $\theta(\xi,0)$ is depicted in Figure 10. It is noted that the higher the value of β, the higher the temperature is in the stretching case, and the lower it is in the shrinking case. By extension, in extension flows, higher β decreases fluid resistance, increases viscous heating, and increases thermal boundary layer, resulting in an increase in temperature. Conversely, in decreasing flows, increased the force opposing the inward movement, and therefore, enhances more heat diffusion, thereby reducing the temperature. Thus, the Casson parameter β is crucial in the regulation of heat transfer in Casson fluid boundary layers at conditions of stretching and shrinking.

Table 1 and Table 2 show the different values of Nu_x and C_f for various values of parameters. Nusselt number enhances by increasing the Prandtl parameters, power law number, radiation number, magnetic number and Casson parameter. Similarly, Skin friction goes up by growing values for magnetic and power law parameters. While decreasing for Casson and suction/injuction number.

IV. CONCLUSION

This paper has numerically examined the radiative magnetohydrodynamic (MHD) Casson fluid flow past a nonlinear extended sheet with suction/injection effect in a non-similarity framework through MATLAB BVP4c method. The acquired findings indicate that physical parameters impacting on the governing flow and thermal behavior are highly affected by Casson parameter, power-law index, magnetic parameter, radiation parameter, suction/injection parameter, and Prandtl number. The velocity field has a decreasing pattern with increasing Casson parameter in the stretching instances but an increasing trend in the shrinking surfaces. The power-law parameter increases velocity in stretching and decreases in shrinking flows, decreases temperature in stretching and increases in shrinking flows. Suction/injection parameter stabilizes the flow and results in velocity increase in extension and velocity decrease in shrinkage. The magnetic parameter inhibits velocity in the stretching but promotes it in the shrinking, whereas it raises the temperature in the stretching and lowers it in the shrinking instances. Thermal radiation lowers the temperature of stretching and raises the temperature of shrinking and the Prandtl number lowers the temperature of stretching and raises the temperature of shrinking. Also, the Nusselt number calculated shows that higher heat transfer rates are made by a greater Pr, m, Rd, xi and beta, and by increasing skin-friction coefficients, and decreasing with increasing beta and S.

ACKNOWLEDGMENT

We acknowledge the organizing committee and all sponsors of 5th International Conference On Frontiers In Academic Research ICFAR 2025 for their dedication and efforts in making this event a success. Their hard work and support are greatly appreciated.

REFERENCES

[1] P. Siddheshwar and U. Mahabaleswar, *Effects of radiation and heat source on MHD flow of a viscoelastic liquid and heat transfer over a stretching sheet,* International Journal of Non-Linear Mechanics, vol. 40, no. 6, pp. 807–820, 2005.

[2] N. S. Wahid, M. E. H. Hafidzuddin, N. M. Arifin, M. Turkyilmazoglu, and N. A. Abd Rahmin, Magnetohydrodynamic (MHD) slip darcy flow of viscoelastic fluid over a stretching sheet and heat transfer with thermal radiation and viscous dissipation, CFD Letters, vol. 12, no. 1, pp. 1–12, 2020.

[3] R. Mahesh, U. Mahabaleshwar, E. H. Aly, and O. Manca, An impact of CNTs on an MHD Casson Marangoni boundary layer flow over a porous medium with suction/injection and thermal radiation, International Communications in Heat and Mass Transfer, vol. 141, p. 106561, 2023.

[4] U. Mahabaleshwar, K. Sneha, and A. Wakif, Significance of thermo-diffusion and chemical reaction on MHD Casson fluid flows conveying CNTs over a porous stretching sheet, Waves in Random and Complex Media, pp. 1–19, 2023.

[5] R. Mahesh, U. S. Mahabaleshwar, and F. Sofos, Influence of carbon nanotube suspensions on Casson fluid flow over a permeable shrinking membrane: an analytical approach, Scientific Reports, vol. 13, no. 1, p. 3369, 2023.

[6] M. Shamshuddin, A. Saeed, S. Mishra, R. Katta, and M. R. Eid, Homotopic simulation of MHD bioconvective flow of water-based hybrid nanofluid over a thermal convective exponential stretching surface, International Journal of Numerical Methods for Heat & Fluid Flow, vol. 34, no. 1, pp. 31–53, 2024.

[7] C.-O. Ng, Combined pressure-driven and electroosmotic flow of Casson fluid through a slit microchannel, Journal of Non-Newtonian Fluid Mechanics, vol. 198, pp. 1–9, 2013.

[8] B. Jalili, A. Rezaeian, P. Jalili, D. D. Ganji, and Y. Khan, *Squeezing flow of Casson fluid between two circular plates under the impact of solar radiation,* ZAMM—Journal of Applied Mathematics and Mechanics, vol. 103, no. 9, p. e202200455, 2023.
[9] M. Hussain et al., MHD thermal boundary layer flow of a Casson fluid over a penetrable stretching wedge in the existence of nonlinear radiation and convective boundary condition, Alexandria Engineering Journal, vol. 60, no. 6, pp. 5473–5483, 2021.
[10] S. Khan, S. Muhammad Imran, and S. Wang, *Diffusion-thermo Effects in Stagnation Point Flow of Second Grade Fluid past a Stretching Plate,* Journal of Applied and Computational Mechanics, vol. 7, no. 2, pp. 902–912, 2021.
[11] S. Khan et al., On the analysis of the non-Newtonian fluid flow past a stretching/shrinking permeable surface with heat and mass transfer, Coatings, vol. 11, no. 5, p. 566, 2021.
[12] K. Nihaal, U. Mahabaleshwar, N. Swaminathan, D. Laroze, and L. Pérez, *Thermal transfer enhancement in a Casson-based hybrid nanofluid flow in a permeable wall jet with suction and injection,* Multiscale and Multidisciplinary Modeling, Experiments and Design, vol. 8, no. 3, p. 163, 2025.
[13] A. H. Ganie, A. M. Mahnashi, A. Shafee, R. Shah, and D. Fathima, Comparative analysis of Casson nanofluid flow over shrinking sheet under the influence of thermal radiation, electric variable, and cross diffusions: Multiple solutions and stability analysis, IEEE Access, 2024.
[14] A. Sumithra, R. Sivaraj, A. J. Benazir, and O. D. Makinde, *Nonlinear thermal radiation and activation energy effects on bioconvective flow of Eyring-Powell fluid,* Computational Thermal Sciences, vol. 13, no. 6, 2021.
[15] P. Yesodha, B. Bhuvaneswari, S. Sivasankaran, and K. Saravanan, *Convective heat and mass transfer of chemically reacting fluids with activation energy with radiation and heat generation,* Journal of Thermal Engineering, vol. 7, no. 5, pp. 1130–1138, 2021.
[16] S. M. Ibrahim, Radiation effects on mass transfer flow through a highly porous medium with heat generation and chemical reaction, International Scholarly Research Notices, vol. 2013, no. 1, p. 765408, 2013.
[17] B. Y. Isah, M. M. Altine, and S. I. K. Ahmad, *Thermal radiation and variable pressure effects on natural convective heat and mass transfer fluid flow in porous medium,* Nigerian Journal of Basic and Applied Sciences, vol. 27, no. 1, pp. 48–58, 2019.
[18] G. Vanitha, R. Jhala, D. Arunkumar, S. Singh, and B. Pattanayak, Heat and Mass Transfer Analysis in Hiemenz Flow of Nanofluid Infused With Carbon Nanotubes in a Micropolar Fluid Model, Heat Transfer, 2025.
[19] M. Khan, M. Sarfraz, R. Zehra, S. M. Hussain, and I. Alraddadi, *Analysis of fluid flow and heat transfer in CNT-infused spiraling disk,* Numerical Heat Transfer, Part A: Applications, pp. 1–12, 2024.
[20] H. Akshatha, S. Sachhin, U. Mahabaleshwar, R. K. Lodhi, and K. Ramesh, *Dynamics of sodium alginate-based ternary nanofluid flow over a stretching sheet with Al_2O_3, SiO_2, and TiO_2 nanoparticles,* Multiscale and Multidisciplinary Modeling, Experiments and Design, vol. 8, no. 1, p. 32, 2025.
[21] M. Saleem, M. N. Tufail, and Q. A. Chaudhry, Unsteady MHD Casson fluid flow with heat transfer passed over a porous rigid plate with stagnation point flow: Two-parameter Lie scaling approach, Pramana, vol. 95, no. 1, p. 28, 2021.
[22] S. Ashraf, M. Mushtaq, K. Jabeen, S. Farid, and R. M. A. Muntazir, Heat and mass transfer of unsteady mixed convection flow of Casson fluid within the porous media under the influence of magnetic field over a nonlinear stretching sheet, Proceedings of the Institution of Mechanical Engineers, Part C: Journal of Mechanical Engineering Science, vol. 237, no. 1, pp. 20–38, 2023.
[23] Y. D. Reddy, B. S. Goud, N. R. Nalivela, and V. S. Rao, Impact of porosity on two-dimensional unsteady MHD boundary layer heat and mass transfer stagnation point flow with radiation and viscous dissipation, Numerical Heat Transfer, Part A: Applications, vol. 85, no. 8, pp. 1172–1190, 2024.
[24] P. Sudarsana Reddy and P. Sreedevi, Impact of chemical reaction and double stratification on heat and mass transfer characteristics of nanofluid flow over porous stretching sheet with thermal radiation, International Journal of Ambient Energy, vol. 43, no. 1, pp. 1626–1636, 2022.
[25] B. Shankar Goud and G. Dharmaiah, *Role of Joule heating and activation energy on MHD heat and mass transfer flow in the presence of thermal radiation,* Numerical Heat Transfer, Part B: Fundamentals, vol. 84, no. 5, pp. 620–641, 2023.
[26] S. Muhammad Raza Shah Naqvi et al., Numerical investigation of thermal radiation with entropy generation effects in hybrid nanofluid flow over a shrinking/stretching sheet, Nanotechnology Reviews, vol. 13, no. 1, p. 20230171, 2024.
[27] T. Naseem, F. Mebarek-Oudina, H. Vaidya, N. Bibi, K. Ramesh, and S. Khan, Numerical analysis of entropy generation in joule heated radiative viscous fluid flow over a permeable radially stretching disk, Computer Modeling in Engineering & Sciences, vol. 143, no. 1, p. 351, 2025.
[28] K. Sneha, U. Mahabaleshwar, M. Sharifpur, M. H. Ahmadi, and M. Al-Bahrani, *Entropy analysis in MHD CNTs flow due to a stretching surface with thermal radiation and heat source/sink,* Mathematics, vol. 10, no. 18, p. 3404, 2022.
[29] M. Nayak, G. Mahanta, M. Das, and S. Shaw, Entropy analysis of a 3D nonlinear radiative hybrid nanofluid flow between two parallel stretching permeable sheets with slip velocities, International Journal of Ambient Energy, vol. 43, no. 1, pp. 8710–8721, 2022.
[30] S. Mandal and G. C. Shit, Entropy analysis of unsteady MHD three-dimensional flow of Williamson nanofluid over a convectively heated stretching sheet, Heat Transfer, vol. 51, no. 2, pp. 2034–2062, 2022.